Sustainable Energy Technologies and Assessments 44 (2021) 101020

Contents lists available at ScienceDirect

Sustainable Energy Technologies and Assessments

journal homepage: www.elsevier.com/locate/seta

Achieving zero-energy building performance with thermal and visual comfort enhancement through optimization of fenestration, envelope, shading device, and energy supply system

Mehrdad Rabani [a,b,*], Habtamu Bayera Madessa [a], Natasa Nord [b]

[a] Department of Civil Engineering and Energy Technology, Oslo Metropolitan University, Norway
[b] Department of Energy and Process Engineering, Norwegian University of Science and Technology, Norway

ARTICLE INFO

Keywords:
Building retrofitting
Optimization process
Shading control method
Window opening control method
Zero energy building

ABSTRACT

Building retrofitting towards nearly zero energy building (nZEB) with comfortable visual and thermal conditions, requires a comprehensive parametric analysis of building retrofit measures. This paper presented an optimization method to automate the procedure of finding the best combination of measures minimizing the building energy use and achieving the nZEB target while enhancing both thermal and visual comfort conditions. The study was performed by coupling of an Indoor climate and energy simulation software (IDA-ICE) and a generic optimization tool (GenOpt) through a Graphical Script interface and the optimization was applied to a typical office building located in Norway. The adopted method allowed the concurrent optimization of building envelope, building energy supply, fenestration, and shading device material, and control methods. Two constraint functions including visual and thermal comfort criteria were considered. Afterwards, PV panels were integrated with the building site for on-site production of electricity towards ZEB level. Findings demonstrated that the inclusive optimization approach could significantly decrease the building energy use, up to 77%, and improve both the thermal and visual comfort simultaneously. Furthermore, the best performance for the optimal solution was achieved when the shading device and window opening control methods functioned with solar radiation and indoor air temperature setpoints.

1. Introduction

Buildings account for a large share of total energy use and significantly contribute to global warming. In the EU, building sector stands for 40% of total energy use [1] and releasing approximately 40% of all GHG emissions [2]. As the total energy use is expected to increase in the future, [3] energy efficiency measures should be considered in different areas such as building sector so that a widespread sustainable development can be achieved. In this regard, the latest update of EPBD requires all EU member states to develop a roadmap for the energy retrofitting of existing buildings [4]. Especially, when the energy savings potential on a national level is the matter of concern, it is essential to investigate the existing building stock due to substantially worse energy performance in older buildings than newer ones [5].

While considering the energy efficiency in buildings, thermal comfort and well-being of occupants are aspects of great significance, especially in office buildings. However, improving both indoor climate and visual conditions may lead to increase in the energy use. It is even more challenging when the target is to improve the building energy performance towards nZEB and to provide thermal and visual comfort at the same time [6,7]. Therefore, a large number of studies have investigated the impact of applying various retrofit measures on the building energy performance through different approaches such as data-driven methods, [8,9] optimization techniques, [10,11] or combination of both approaches [12,13]. Data-driven methods, which are also referred as grey-box or black-box models, take advantage of statistical analysis to find the relationships between the building input and output variables without detailed knowledge of building physical behavior [12]. However, optimization approaches adopt machine learning techniques and algorithms such as genetic algorithm, particle swarm optimization, and sequential search to find the optimal set of building retrofit measures through an iterative process, [14] which was considered in this study.

* Corresponding author at: Department of Civil Engineering and Energy Technology, Oslo Metropolitan University, Norway.
E-mail addresses: Mehrdad.Rabani@oslomet.no (M. Rabani), Habtamu-Bayera.Madessa@oslomet.no (H. Bayera Madessa), natasa.nord@ntnu.no (N. Nord).

https://doi.org/10.1016/j.seta.2021.101020
Received 23 September 2020; Received in revised form 16 December 2020; Accepted 12 January 2021
Available online 1 February 2021

Nomenclature

Roman symbols

A	area of each zone (m^2)
A_{eff}	effective area of the window opening (m^2)
AHU	air handling unit
ANN	artificial neural network
C_d	discharge coefficient
CAV	constant air volume
CFD	computational fluid dynamics
DF_{avg}	average daylight factor
DH_{26}	discomfort hours for the indoor operative temperature more than 26 °C during occupancy (h)
DHW	domestic hot water
$E_{el.prod}$	produced electricity by PV cells (kWh)
$E_{el.use}$	energy use due to lighting, equipment, HVAC system and domestic hot water (kWh)
E_{imp}	imported energy (kWh)
E_{exp}	delivered energy to the grid (kWh)
$E_{P,exp}$	primary exported energy (kWh)
$E_{P,imp}$	primary imported energy (kWh)
$E_{self,use}$	self-consumption of generated electricity (kWh)
E_{tot}	specific total delivered energy to the building on annual basis (kWh/(m^2·year))
EPBD	energy performance of buildings directive
EU	European Union
GA	genetic algorithm
GenOpt	generic optimization program
GHG	greenhouse gas
GS	graphical script
GSHP	ground-source heat pump
H	window height (m)
HVAC	heating, ventilation, air conditioning system
i	type of energy carrier
k	zone counter
LCC	life cycle cost
MOBO	multi-objective building optimization
m	monthly/hourly counter
N	total number of zones
NSGAII	non-dominated sorting genetic algorithm II
n_{50}	airtightness
nZEB	nearly zero energy building
PDH	total occupant hours dissatisfaction
PH	passive house
PMV	predicted mean vote
PPD	predicted percentage dissatisfied (%)
PPD_{avg}	annual average of predicted percentage dissatisfied during total occupied hours (%)
PR	performance ratio relating the actual and the theoretical energy output of the PV system
PSO	particle swarm optimization
PV	photovoltaic
Q_{sol}	solar radiation for controlling shading (W/m^2)
SFP	specific fan power (kW/(m^3/s))
U	total heat transfer heat coefficient (W/(m^2·K))
UDI	useful daylight illuminance
VAV	variable air volume
W	window width (m)
W_DH_{26}	weighted discomfort hours
W_PPD	weighted predicted percentage of dissatisfied
w	weighting factors/metrics for primary energy
ZEB	zero energy building

Greek symbols

ψ	normalized thermal bridge (W/(m^2·K))
γ	mismatch factor/supply cover factor (%)

2. Literature review on the optimization of building energy performance

2.1. Building envelope and HVAC setpoints

In order to facilitate the process of finding the optimal set of building retrofit measures, many studies have suggested an optimization approach. In this respect, numerous studies focused on the optimization of building envelope, façade parameters, and the setpoints for space heating, space cooling, and ventilation system. Table 1 shows a summary of these parameters applied in the most recent studies.

2.2. Parameters of building energy supply system

Studies in the literature also showed that optimizing the type and parameters of the building energy supply system could improve the building performance. Lu et al. [27] investigated single and multi-objective optimization of PV cell size, wind turbine size and power, and the capacity of bio-diesel generator in order to minimize the total cost of renovations, CO_2 emissions, and building-grid interaction index. Wu et al. [28] optimized the operation strategies for energy conversion and storage technologies including heat pumps, solar panels, biomass, oil boilers and thermal storage in order to minimize the annualized costs and life cycle GHG emissions of typical residential buildings. Hirvonen et al. [29] performed a multi-objective optimization process to minimize the LCC and CO_2 emissions due to the renovation of four Finish reference buildings. In addition to building envelope characteristics and window type, they considered energy system parameters including type and capacity of heat pump, PV size, and the type of sewage heat recovery system from wastewater. The results showed that utilizing the GSHP as the energy supply system was the most cost-effective renovation measure. Ferrara et al. [30] investigated the optimization of building envelope and energy supply system in order to minimize the global cost during the entire life cycle of the building. The energy supply parameters consisted of the choice of generator terminals, auxiliary heaters for domestic hot water, PV type, dimension of water storage, and the percentage of building roof area covered by PV and thermal solar collectors.

2.3. Visual comfort parameters

Since optimizing building fenestration and glazing is always accompanied by compromising the occupants' visual comfort, some studies investigated the optimization of the visual comfort either by maximizing it as an objective function or considering it as a constraint function. Taveres-Cachat et al. [31] optimized the angle of louver blades and their center point coordinate in a PV integrated shading system to minimize the total net energy use, maximize the daylight level and the energy converted by the PV material. Fang and Cho [32] conducted an optimization study including the combined effects of window size, skylight size and location, and length of horizontal fixed sun louver on the maximization and minimization of UDI and energy use intensity, respectively. Pilechiha et al. [33] proposed an optimization framework for maximizing the daylight and minimizing the building energy use. The size of windows and room dimensions were altered during the optimization. The results showed a possibility of providing satisfactory quality of view for more than 80% of the reference room points, considering maximizing and minimizing the building daylight and energy use, respectively [20]. Kirimtat et al. [34] presented a detailed

Table 1
Type of building envelope, façade parameters, and HVAC setpoints included in the optimization design variables in recent scientific studies.

Authors	Description	Design variables
Rosso et al. [15]	A multi-objective optimization was proposed to minimize building energy use, construction and energy costs, and CO_2 emission. EnergyPlus was coupled with Python for the novel genetic algorithm aNSGA-II.	• Glazing system • Radiative properties of finishing layer • Vertical and horizontal insulation thickness • Presence or absence of solar shading • Change open balconies into glazed, movable sun spaces, closed during the cold season
Lu et al. [16]	A reliability analysis was conducted on the optimization of office buildings under uncertainties in the envelope and occupancy parameters. Rhinoceros, EnergyPlus, and the genetic algorithm were integrated for this purpose.	• U-value of walls • Visible transmittance of window
Ascione et al. [17]	A tailored rating assessment approach, comprised of optimization, validation, analysis and planning of requalification interventions, was carried out to improve the performance of an industrial building in terms of primary energy consumption and global cost. The optimization was done through coupling between EnergyPlus and MATLAB.	• Type of window • Presence and absence of solar screen • Heating temperature setpoint schedule • HVAC air flow rates
Chang et al. [18]	A multi-objective optimization framework was developed to minimize the energy use, indoor thermal discomfort, CO_2 emissions, and payback period in residential buildings. EnergyPlus was coupled with GA, which modelled in MATLAB, for optimization process.	• Vertical façade option including Trombe wall, double skin façade, solar PV, PCM integrated in wood-lightweight concrete, and Algae façade • Roof options including exterior metal roof, green roof, solar PV, and cool coated roof
Li and Wang [19]	A coordinated multi-stage optimizations of building design and energy systems was proposed as a computation cost-effective method for zero/low energy buildings. An ANN model and a GA-based using EnergyPlus was adopted.	• Roof solar absorptance • Window-to-wall ratio • Wall solar absorptance • Overhang projection ratio
Si et al. [20]	A multi-objective optimization was applied to the design of a newly built complex building. The aim was to minimize annual energy demand and average predicted percentage dissatisfied. Simulations were done using EnergyPlus integrated with modeFRONTIER for automatic runs and parallel simulations.	• Exterior wall insulation thickness and conductivity • Roof insulation thickness and conductivity • Exterior window type • Cooling and heating temperature setpoints
Ascione et al. [21]	A multi-objective optimization was implemented through coupling between EnergyPlus and MATLAB to minimize the building primary energy use and global cost of retrofit measures in two different climates.	• Roof insulation thickness • Vertical walls insulation thickness • Window type • Position of the shading systems • Percentage of the roof covered by photovoltaic panels
Ascione et al. [22]	A multi-optimization framework was proposed to minimize the daily running cost of space heating and maximum PPD over a specific day via weather-data-based control for residential buildings. EnergyPlus and MATLAB were coupled for this purpose.	• Heating setpoint temperature during a hourly interval of the investigated day for different thermal zone type
Ilbeigi et al. [23]	A single-objective optimization was carried out to minimize the energy use of an office building by coupling EnergyPlus with Galapagos plugin based on a Genetic Algorithm.	• Wall U-value • Infiltration rate • Roof U-value
Bui et al. [24]	An optimization of building performance was carried out to minimize the energy use of a simple office model by applying an adaptive facade. EnergyPlus was linked to Eppy toolkit in Python.	• Adaptive façade using an electrochromic window. • Window visible transmittance • Window U-value
Nasruddin et al. [25]	A two-objective optimization approach was implemented to minimize building energy use and maximize thermal comfort through the improvement of HVAC system. IESVE software (for energy simulation and PPD calculations) was coupled with ANN and a multi-objective GA.	• Cooling setpoint • Relative humidity setpoint • Supply air flow rate (VAV system) • Window area • Wall thickness • Supply air temperature (VAV system) • Supply radiant temperature (radiant system) • Supply radiant flow rate (radiant system) • Starting and stopping thermostat delay
Guo et al. [26]	An optimization framework was developed to minimize the total building cooling energy use and maintain the PPD at certain level through improvement of night ventilation system control. EnergyPlus was linked to Omni-optimizer.	• Night venting duration • Minimum indoor temperature setpoint • Night air change rate setpoint • Activation threshold temperature • Internal thermal mass area • Specific fan power

optimization study on the design alternatives of a shading device with amorphous cells in order to minimize the total energy use and maximize the UDI of a test room model. For each shading panel, the shading distance from the window, movement point and rotation angle of shading slats were optimized. Yi [35] performed an optimization study on the geometry elements of an amorphous building façade to improve its daylighting performance. The aim was to find the best user's design preference in order to qualitatively and quantitatively improve the building visual performance and aesthetic value simultaneously. Naderi et al. [36] optimized the architectural features and control parameters of a smart shading blind in a simple room to improve both visual and thermal comfort conditions. The design parameters included the slat width, angle, thickness, and reflectance, blind distance to the glass, shading location (interior, exterior), and shading control strategies. They adopted average discomfort glare index as the objective function for visual comfort.

2.4. Thermal comfort parameters

Occupant's thermal comfort is also another conflicting barrier in improving the building energy performance and it has been addressed in various ways. Magnier and Haghighat [37] considered thermal comfort as an objective function to be maximized along with the total energy use to be minimized simultaneously. They used average and absolute PMV as the thermal comfort objective. Hong et al. [38] used PMV also as the thermal comfort objective function to be minimized along with the energy use, the net present value, and the global warming potential of building renovation measures. Grygierek and Ferdyn-Grygierek [39] conducted an optimization study to minimize the life cycle cost of

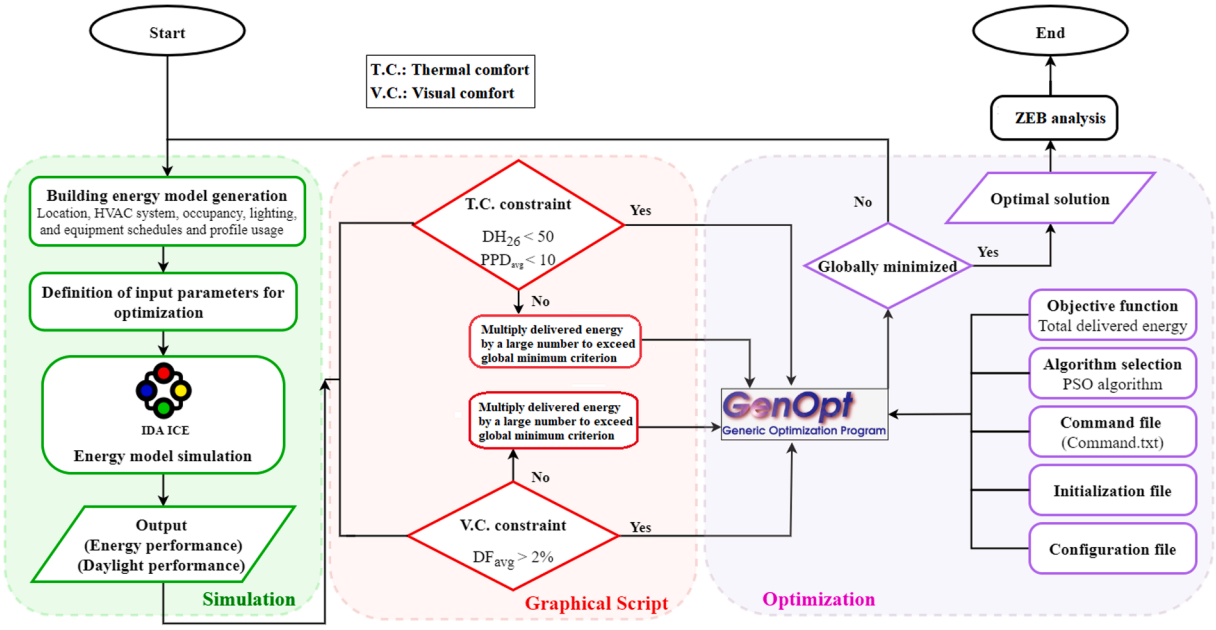

Fig. 1. Proposed framework for the optimization process.

building retrofitting measures and maximize the thermal comfort of occupants at the same time. Maximizing the thermal comfort of occupants was, in fact, done by minimizing the number of thermal discomfort hours. Niemelä et al. [40] proposed a multi-objective optimization to minimize the three objectives: CO_2 emissions due to delivering energy to the building, the net present value of its life cycle cost, and the PDH. Sghiouri et al. [41] performed an optimization study to minimize an area-weighted mean discomfort degree-hours by modifying the overhangs projections of a building case. Ascione et al. [11,42,43] in three different multi-optimization frameworks considered the annual percentage of discomfort hours over occupied hours as the thermal comfort objective function to be minimized along with other objectives. The discomfort hours were assessed when PPD was higher than 20%.

2.5. Building energy simulation and optimization tools

There are several building energy performance and optimization tools frequently used in literature for building performance and optimization purposes. Regarding optimization tool, Tian et al. [44] carried out a review on the existing optimization tools, namely, GenOpt, [45] MOBO, [46] jEPlus + EA, [36,47] BEopt, [48] and MultiOpt [49] tools. These tools were integrated with building energy performance simulation tools such as EnergyPlus, [50–52] TRNSYS, [7,49,53] and IDA-ICE [29,40,54].

The aforementioned studies highlighted the importance of considering a hybrid set of building envelope and HVAC system parameters in the optimization process in order to improve the building energy performance and satisfy the visual and thermal comfort of occupants at the same time. Nevertheless, various shading and window opening control strategies, and HVAC setpoints were not studied together during optimizations in the literature. Therefore, the novelty of our paper was to investigate the interaction of window opening and shading device automatic control methods and parameters with other important design variables through optimization process, which was missing in the literature. Various control strategies and setpoints for shading devices, window opening and HVAC system can be conflicting when reducing building energy use and satisfying thermal and visual comfort conditions simultaneously. This was accomplished by integrating the IDA Indoor Climate and Energy (IDA-ICE) software and optimization tool (GenOpt) in order to improve the energy performance of a typical existing office building and to find out what the minimum energy use would be considering both visual and thermal comfort conditions.

In the following sections, the proposed simulation-based method for a typical Norwegian office building is described. In this respect, the base case design configuration, conditions, and HVAC system, and setpoints are introduced. Afterwards, a wide range of parameters including building envelope, window glazing type, window to floor area ratio, and control strategies and setpoints for shading devices, window opening, and HVAC system are given. Besides, a PV is added in order to balance the total building energy use to achieve the ZEB level in the optimal solutions. Afterwards, the obtained results for the optimal cases are presented and commented. Finally, the main conclusions are summarized and the possibilities for the future work are discussed.

3. Method

Fig. 1 illustrates the proposed method for this study. The method was structured in several steps:

- The pre-processing step (the green area in Fig. 1), in which the building model was generated in IDA-ICE and the input parameters for the optimization problem were defined.
- The intermediate step (the red area in Fig. 1), where the output parameters from the energy simulation software were evaluated in terms of DF_{avg}, DH_{26}, and PPD_{avg}. The first parameter, daylight factor, was considered as the visual comfort index and the two latter, discomfort hours for the indoor operative temperature more than 26 °C and predicted percentage dissatisfied, were chosen as the thermal comfort indexes.
- The optimization step (the purple area in Fig. 1), where the objective function was iteratively assessed until an optimal solution was achieved.
- The post-processing step (the "ZEB analysis" box in Fig. 1), where the optimal solutions were elaborately analyzed in terms of ZEB balance.

3.1. Pre-processing step

In the pre-processing stage, the building energy model was generated in IDA-ICE software.

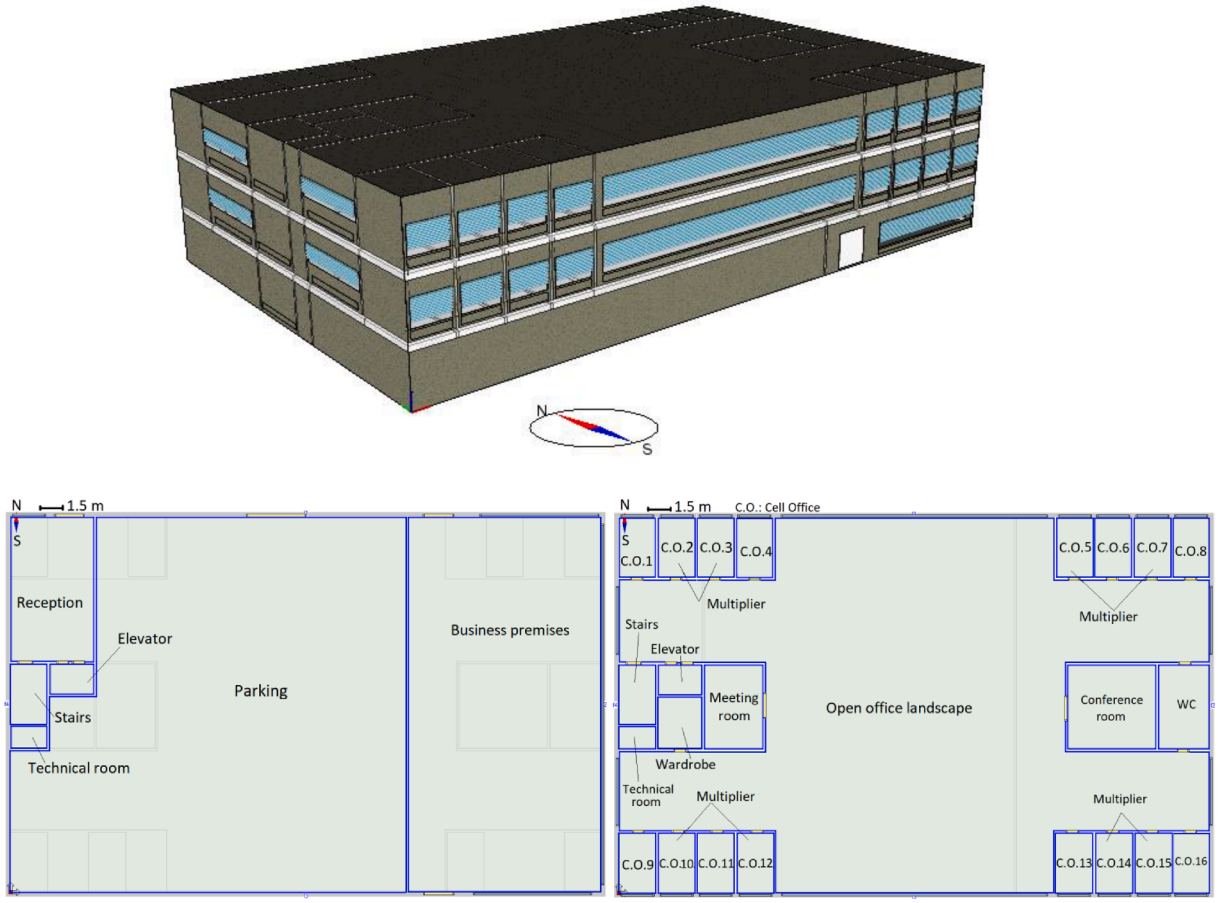

Fig. 2. Office building configuration (top), the first floor plan (bottom-left), and the second and the third floor plans at level 3.4 m and 6.8 m (bottom right).

Table 2
General building information on the reference case.

Parameter	Value/Feature
Building orientation	North-South
Number of floors	3
Floor height (m)	2.9
Total building height (m)	10.5
Total heated floor area (m^2)	2 940
Total building volume (m^3)	9 062
Total window area (m^2)	286.2
Total door area (m^2)	21

Table 3
Properties of the building envelope for the reference case.

Parameter, Units	Value
External wall U-value, W/(m^2K)	0.3
Roof U-value, W/(m^2K)	0.2
Floor U-value, W/(m^2K)	0.2
Window U-value, W/(m^2K)	2.4
ψ, W/(m^2·K)	0.13
n_{50}, 1/h	4
External door U-value, W/(m^2K)	2
External shading strategy	Blinds on, if Q_{sol} > 100 W/m^2 [57]

3.1.1. Case study and building energy model generation

We considered a case study model representing the configuration of typical office buildings located in Norway. According to the statistics of office building stock in Norway, most of office buildings were built in the 1980 s with a total heated floor area between 2,500 to 10,000 m^2 [55]. Therefore, as a case study, a reference office building with 3,000 m^2 total heated floor area was considered for the simulations in this study. The building envelope characteristics, lighting system, and HVAC system, and setpoints were chosen for a typical office building constructed in 1987 satisfying the Norwegian building code TEK87 [56]. Fig. 2 shows the office building model developed in IDA-ICE. "Multiplier" in Fig. 2 presents the zone multiplier, which is an available function in IDA-ICE, used to simplify the duplicate cell offices in the second and the third floors in order to reduce the simulation computational time. Furthermore, the type of shading device for the windows was an exterior venetian blind. The general building information about the reference case building are given in Table 2. The total window area was selected based on TEK87, so that the window to floor area ratio did not exceed 15%.

Table 3 presents the building envelope properties of the reference building. All characteristics were considered according to the Norwegian building code TEK87. The HVAC system parameters and setpoints and usage profiles for the reference case are shown in Table 4. In addition, DHW use was selected according to the Norwegian standard NS 3031 [57].

Table 5 presents the internal heat gains due to occupancy, lighting, and equipment along with their usage profiles. As the reference building was built in 1987 and is currently in use, the internal heat gain due to equipment and its usage profile was implemented in IDA-ICE according to the Norwegian standard NS 3031. Furthermore, a measurement-based data of several cell offices in an office building in Norway [58] was considered to have a realistic pattern of lighting and occupancy behavior, as shown in Fig. 3.

The simulations were run over a period of one year with the typical weather data taken from the ASHRAE IWEC 2 database for Oslo, Norway climate. The annual mean outdoor temperature was around 6.3°C and

Table 4
Characteristics of the HVAC system in the reference building.

HVAC systems and operation	Features
Ventilation system type	CAV mechanical balanced ventilation system
The SFP of the ventilation system	2.5 kW/(m^3/s)
Schedules of ventilation system	Monday-Friday: 12 h/day for upper limit (6–18); other times reduces to lower limit
Supply airflow rates of the ventilation system	Primary zones: 4.32 m^3/(m^2.h) and 19.8 m^3/(m^2.h) for upper limit in heating and cooling seasons respectively, 0.72 m^3/(m^2.h) for lower limit Secondary zones: 2.52 m^3/(m^2.h) for upper limit, 0.72 m^3/(m^2.h) for lower limit
Heating system	Central heating system, modelled in IDA-ICE using a generic electric heater with unlimited capacity and efficiency of 90%
Cooling system	Centralized water cooling system for cooling of supply air in the AHU
Heating distribution system	Water radiator system
Room temperature setpoint for local space heating *	19℃ for heating
Control method of space heating and ventilation air heating and cooling systems	Space heating: supply water temperature as a function of outdoor temperature; Ventilation supply air temperature: as a function of outdoor temperature;
DHW use	5 kWh/(m^2.year)

* There was no local space cooling system in the zones and cooling of zones was done by the mechanical ventilation system.

Table 5
Internal heat gains and usage profiles due to occupancy, lighting, and equipment.

Usage profile of internal heat gains	Source values of internal heat gains
- Occupants, the usage profile was considered based on measurement data.	Each person occupies around 10 m^2 of floor area, with activity level is 1.2 met, which is equal to 0.1 occupant/m^2
- Lighting, the usage profile was considered based on measurement data.	8 W/m^2
- Office equipment, the usage profile was: Monday-Friday: usage during 6–18o'clock, no usage at other times including weekends and holidays. No equipment for secondary zones	11 W/m^2

the space heating design outdoor temperature was considered around −20℃. Further detail about the climatic condition for this city can be found in ASHRAE classification [59]. It should be underlined that the building model in this study matched the requirements of Norwegian building code TEK 87 for specific annual energy needs of office buildings, as reported in [5].

3.1.2. Definition of input parameters for optimization

In total, 15 input variables in three main categories were considered for the optimization as shown in Table 6. The first group of variables associated with the building envelope were chosen based on the most relevant parameters in the literature. The insulation materials, applied for the external wall and the roof, were replaced by new insulation materials with different thickness, as shown in Table 6. The second group in the variables corresponded to the HVAC parameters and setpoints. It should be mentioned that overheating in Table 6 means that the supply water temperature for the space heating at central heating system was slightly increased in the morning to avoid a very high peak load. The third group of variables consisted of different control methods for shading devices and window opening. To recall, the optimization latter variables in combination was missing in literature and none of the studies considered the combined control of these two types of variables for the optimization process. The shading material properties are explained in detail in the Appendix (see Table 8). It should be underlined

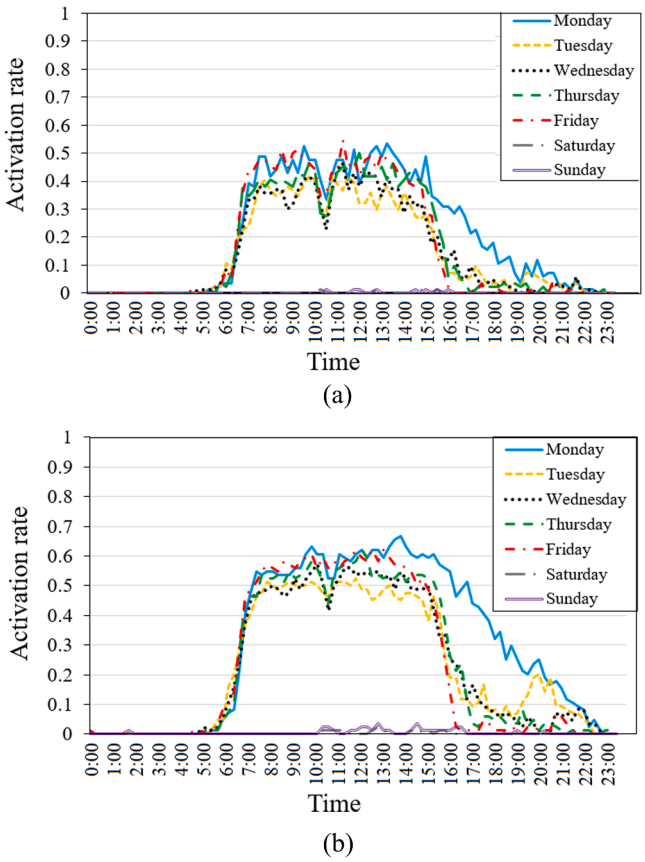

Fig. 3. Average (a) occupancy and (b) lighting patterns for weekdays and weekends.

that in order to implement the window to floor area ratio as a single parameter and place all the windows in the center of the walls, the window coordinates were calculated and adjusted by linking them to this ratio through the GS interface. This was important as the daylight and energy simulations were simultaneously performed in each iteration during the optimization.

The two control methods for the window opening and the six control methods for shading device are illustrated in detail in Fig. 4. It should be noted that both window opening and shading device control methods were controlled and operated automatically. In the window opening control method, the following principles were implemented:

- Condition (a): Indoor air temperature control method was used for the summer and winter operation. The summer operation control was based on indoor operative temperature. The winter operation was based on CO_2 and indoor operative temperature control methods.
- Condition (b): Indoor air temperature control method was combined with the direct solar radiation on the façade and wind velocity control for the summer operation.

It has to be stressed that the window opening in IDA-ICE was applied according to the CELVO model, which defined the window opening area in terms of height, width, and discharge coefficient of the window [60]. The corresponding equation is elaborated in the Appendix (Eq. (10)).

In the shading control methods, the control parameters and rules were implemented as follows:

- Condition (c): Shading position control was suggested with respect to the indoor air temperature outside the working hours (zone not in use) and according to illuminance during the working hours (zone in

Table 6
Optimization parameters considered for the optimization process.

Parameter	Value	Description
Glazing and building envelope		
Window to floor area ratio	(10–24)	Interval: 2.8
Window type	(2.4, 2.2, 2.0, 1.8, 1.6, 1.4, 1.2, 1.0, 0.8,	2.4 based on TEK87 and 0.8 based on NS 3701
(U-value W/(m^2.K))	0.6)	
Roof type	0.20	180 mm EPS S80 insulation
(U-value W/(m^2.K))	0.18	200 mm EPS S80 insulation
	0.16	230 mm EPS S80 insulation
	0.13	280 mm EPS S80 insulation
	0.10	370 mm EPS S80 insulation
	0.08	460 mm EPS S80 insulation
	0.06	620 mm EPS S80 insulation
External wall type	0.30	30 mm Mineral Wool insulation
(U-value W/(m^2.K))	0.28	63 mm Mineral Wool insulation
	0.26	73 mm Mineral Wool insulation
	0.24	83 mm Mineral Wool insulation
	0.22	93 mm Mineral Wool insulation
	0.20	118 mm Mineral Wool insulation
	0.17	150 mm Mineral Wool insulation
	0.15	170 mm Mineral Wool insulation
	0.13	180 mm Mineral Wool insulation
	0.12	230 mm Mineral Wool insulation
	0.10	280 mm Mineral Wool insulation
HVAC parameters and setpoints		
Profile of supply air temperature set pints in AHU (℃)	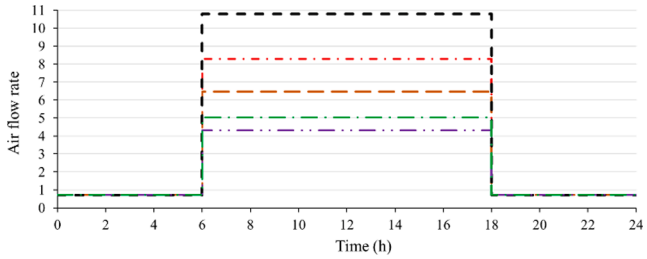	
Profile of supply water temperature setpoints from the central heating system (℃)	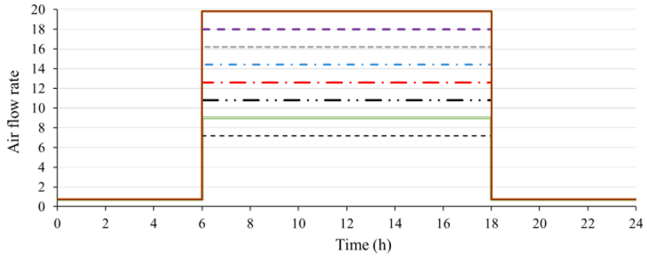	
Supply/return water temperature to/from radiators (℃)	(45, 55,65, 70)/(25, 30, 35, 40)	Sixteen combinations of supply/return temperatures are possible
Heat exchanger efficiency in AHU	(0.55, 0.75, 0.85)	NA
Overheating of zone hot water supply in the central heating system (℃)	1	Always off
	2	5℃ overheating 5–6 AM
	3	9℃ overheating 5–6 AM
	4	5℃ overheating 4–6 AM
	5	9℃ overheating 4–6 AM
Upper/lower limit of ventilation supply airflow rate during heating season (m^3/(h.m^2))	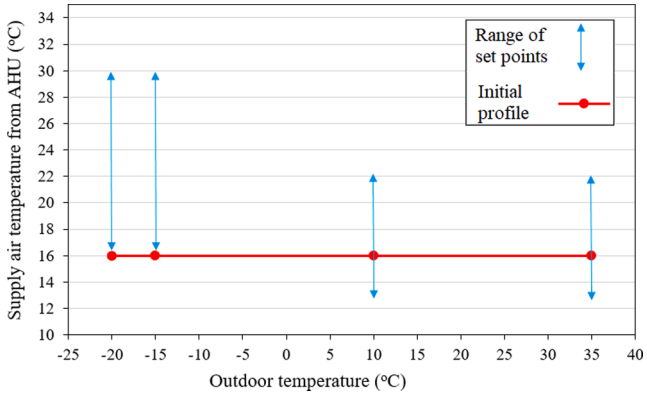	
Upper/lower limit of ventilation supply airflow rate during cooling season (m^3/(h.m^2))		

(*continued on next page*)

Table 6 (*continued*)

Parameter	Value	Description
	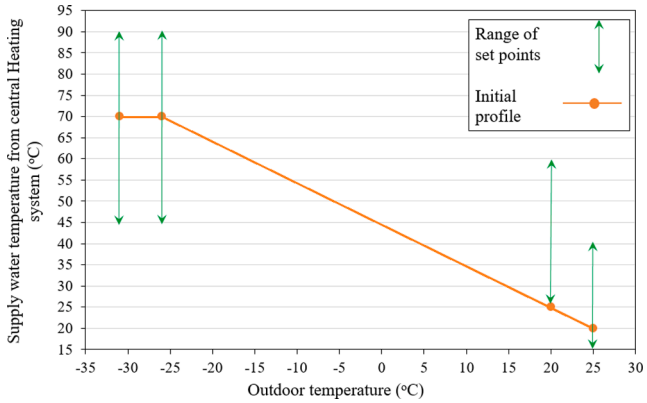	
Shading device and window opening control methods		
Window opening control alternatives	1	Never open
	2	Seasonal opening with temperature and CO_2 control, in Fig. 4 (a)
	3	Opening with temperature and solar radiation control, in Fig. 4 (b)
Shading device control alternatives	1	Never drawn
	2	Daylight-Sun-Min energy, in Fig. 4 (c)
	3	Sun-Get heat, in Fig. 4 (d)
	4	Daylight-Get heat-Min cool, in Fig. 4 (e)
	5	Sun-Get heat-Preserve heat, in Fig. 4 (f)
	6	Daylight control, in Fig. 4 (g)
	7	Solar radiation control, in Fig. 4 (h)
Other parameters		
Lighting rate (W/m^2)	(7, 11, 30)	NA
Shading material type	1	Generic outside blind slat
	2	Marine venetian blind slat
	3	Celery venetian blind slat
	4	Opaque light-dark colored slat
	5	Pewter venetian blind slat
	6	Opaque white colored slat
	7	Mocha venetian blind slat
	8	Bisque venetian Blind slat
	9	White venetian Blind slat

use). It should be pointed out that Condition (c) was the only condition in which the shading slat angle was controlled according to illuminance and changed based on the solar azimuth angle. Otherwise, the slat angle was kept constant at 45° in other conditions. The aim was to minimize energy use and maximize comfort.

- Condition (d): Shading position control was based on the solar radiation measured on the exterior side of windows during the working hours and according to solar radiation and indoor air temperature outside the working hours. The aim was to avoid overheating during working hours and to gain heat outside the working hours.
- Condition (e): Shading position control was based on illuminance during the working hours and according to the indoor air temperature and the minimum solar radiation outside the working hours. The aim was to maximize comfort and minimize mechanical cooling.
- Condition (f): Shading position control was based on the solar radiation measured on the exterior side of windows during the working hours and according to the indoor air temperature and the minimum solar radiation outside the working hours. The aim was to avoid overheating during the working hours and preserve heat gain outside the occupancy hours.
- Conditions (g) and (h): Shading position control was based on illuminance and solar radiation on the exterior side of windows all day long, respectively.

It should be stated that all the algorithms were developed through detailed macros in IDA-ICE as shown in Fig. 4.

3.1.3. Daylight and energy simulation tools

The energy simulations of the optimization analyses were carried out by using the IDA-ICE dynamic simulation. The daylight simulations were performed in the Radiance tool, [61] which was already integrated with IDA-ICE software through the Daylight-tab in the software. In this regard, IDA-ICE employed the Radiance's genBSDF program to assess the solar bidirectional properties of the complex fenestration system with controllable shading. Furthermore, the daylight factor index was used in the simulations with high precision, and the daylight was measured at desktop level. It should be clarified that both energy and daylight simulations in each iteration during optimization process were performed simultaneously in IDA-ICE.

3.2. Intermediate step

3.2.1. GS interface

In implementing the optimization process, an intermediate step was applied in order to arrange the results according to the thermal and visual comfort constraints. The process was done through the GS interface, which is an available option in IDA-ICE (see the central red part in Fig. 1). This module gives the possibility to manipulate the data in an illustrative way by inserting and connecting different components [62]. It should be mentioned that the GS module is executed by IDA modeler without running the IDA solver. In the present work, it was adopted to check the constraint functions during optimization process. If the results of daylight and thermal comfort simulations obtained from IDA to ICE did not satisfy the visual and thermal comfort constraints, the total

Table 7
Optimized input parameters, except HVAC setpoint at AHU and central heating system, for different optimized cases.

Parameters	Min W_PPD when $W\_DH_{26} < 50$	Min E_{tot} when $W\_DH_{26} < 50$	Max DF_{avg} when $DF_{avg} > 2\%$	Min E_{tot} when $DF_{avg} > 2\%$	Global optimal solution
Window to floor area ratio	14.18	14.57	24.00	14.96	14.96
Window (U-value, W/(m^2K))	1.0	0.6	0.6	0.6	0.6
Roof (U-value, W/(m^2K))	0.06	0.06	0.2	0.08	0.08
External wall (U-value, W/(m^2K))	0.1	0.1	0.3	0.1	0.1
Supply/return water temperature to/from radiators (°C)	65/30	70/40	65/35	70/30	70/30
Heat exchanger efficiency in AHU	0.85	0.85	0.85	0.85	0.85
Overheating of zone hot water supply in the central heating system (alternative number in Table 6)	2	2	1	5	5
Window opening control (alternative number in Table 6)	1	3	1	3	3
Shading device control (alternative number in Table 6)	2	5	7	7	7
Lighting rate (W/m^2)	7	7	7	7	7
Shading material type (alternative number in Table 6)	9	9	7	8	8

delivered energy, E_{tot}, would be multiplied by a large number. Therefore, the undesirable results were removed from the acceptable set of solutions as the objective was to minimize the total delivered energy to the building. In addition, this simple method could expedite the process of finding the optimized set of input parameters, selected by the GenOpt tool in each iteration.

3.2.2. Constraint functions implementation

For the purpose of this study, a single objective function, which was $E_{tot,}$ along with two constraint functions for thermal comfort and one for visual comfort were considered for optimization. The constraint functions were DF_{avg}, considered as the visual comfort requirement, and W_DH_{26} and W_PPD, selected as the thermal comfort criteria. The two latter were calculated as follows:

$$W\_DH_{26} = \frac{\sum_{k=1}^{N} A_k . DH_{26k}}{\sum_{k=1}^{N} A_k} < 50\ hours \quad (1)$$

$$W\_PPD = \frac{\sum_{k=1}^{N} A_k . PPD_{avg.k}}{\sum_{k=1}^{N} A_k} < 10\% \quad (2)$$

It should be emphasized that PPD in Eq. (1) was calculated as an average value for each thermal zone in IDA-ICE. Furthermore, the 50 h and 10% criteria in Eqs. (1) and (2) are considered based on the current requirement for the Norwegian building code TEK17 [63] and the requirement for indoor air quality according to the comfort category II [64]. The criterion for average daylight factor was considered $DF_{avg.} > 2\%$, according to the Norwegian building code TEK17 [63] and it was calculated and averaged for the office cubicles. It should be noted that the technical requirements in the Norwegian building code TEK17 are similar as for the PH standard [5].

3.3. Optimization method and tool

In this stage, the optimization process was initiated in the GenOpt engine. Regarding the optimization specifications, in the present study, PSO algorithm was chosen from the GenOpt algorithm library to handle both continuous and discrete input parameters and benefit the global features of the PSO algorithm [45]. The details of parameters for the optimization algorithm are described in the Appendix (see Table 9). The optimization simulations were run on a 32 GB RAM of a Windows-based workstation (2.20 GHz) with Intel (R) Xeon (R) Gold 5120 CPU with 14 parallel cores and lasted for around 40 days to accomplish the whole optimization case.

3.4. Post-processing step

After finding the optimal solution, a ZEB analysis was performed. There are already several ZEB definitions. However, a common approach for all definitions is the annual balance between the weighted demand and the weighted supply [65,66] and it is generally done by integrating PV cells to the building façade and roof. The weighted demand and supply can be calculated in different ways; the export/import balance, load/generation balance, and monthly net balance, which is the combination of two other methods [66,67]. In the present work, the export/import balance method was selected and calculated as follows:

$$ZEB = \left|E_{P,exp}\right| - \left|E_{P,imp}\right| \approx 0 \quad (3)$$

$$E_{P,imp} = \sum_{i} E_{imp}(i) \times w(i) \quad (4)$$

$$E_{P,exp} = \sum_{i} E_{exp}(i) \times w(i) \quad (5)$$

where w is the weighting factors/metrics used in this paper as the primary energy factor and i refers to different type of energy carrier. It should be mentioned that the export/import balance in this study took into consideration the self-consumption of generated electricity, and afterwards created a balance between the need for exported and imported energy as follows:

$$\begin{cases} E_{exp} = \left|\sum_{m=1}^{12}\left(E_{el.use} + E_{el.prod.}\right)\right| & \text{if } \sum_{m=1}^{12}\left(E_{el.use} + E_{el.prod.}\right) < 0 \\ E_{exp} = 0 & \text{if } \sum_{m=1}^{12}\left(E_{el.use} + E_{el.prod.}\right) \geqslant 0 \end{cases} \quad (6)$$

$$\begin{cases} E_{self,use} = \left|\sum_{m=1}^{12} E_{el.prod}\right| & \text{if } \sum_{m=1}^{12}\left(E_{el.use} + E_{el.prod.}\right) > 0 \\ E_{self,use} = \sum_{m=1}^{12} E_{el.use} & \text{if } \sum_{m=1}^{12}\left(E_{el.use} + E_{el.prod.}\right) \leqslant 0 \end{cases} \quad (7)$$

$$E_{imp} = \sum_{m=1}^{12} E_{el.use} - E_{self,use} \quad (8)$$

where m is the number of months or hours for monthly or hourly calculations, respectively.

Finally, the mismatch factor or so called supply cover factor, was calculated as follows [68]:

(a) Window opening: Indoor air temperature control for summer operation and its combination with indoor CO_2 control for winter

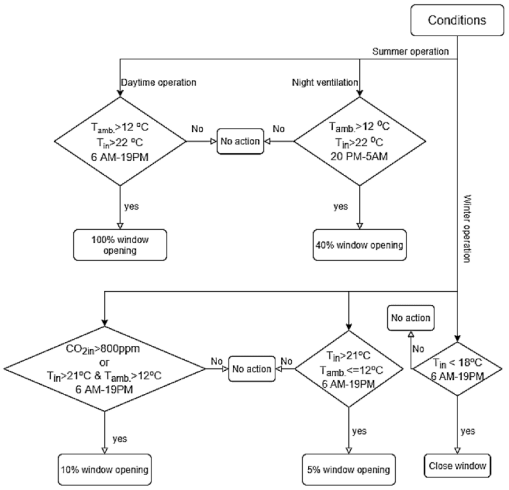

(b) Window opening: Hybrid method through control of indoor air temperature, direct solar radiation on the façade, and wind velocity for summer operation.

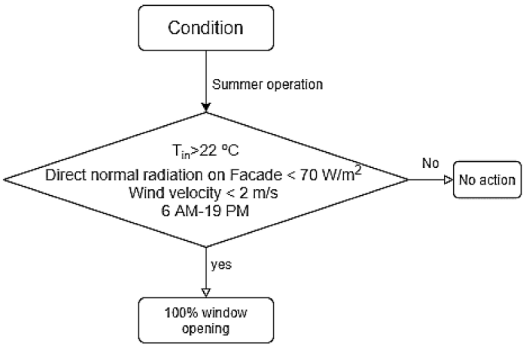

(c) Shading device: Position and slat angle control based on indoor air temperature, illuminance, and working hours

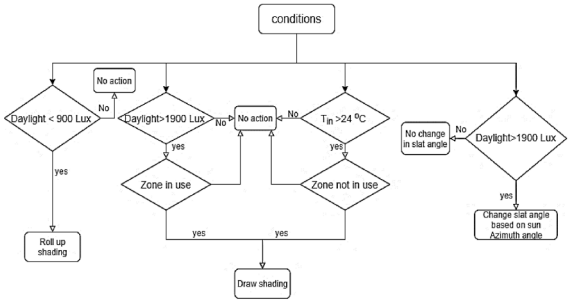

(d) Shading device: Position control based on solar radiation measured on the exterior side of windows, indoor air temperature, and working hours

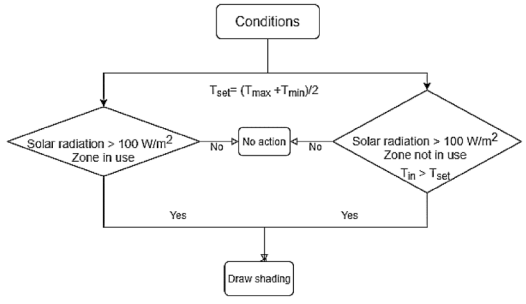

(e) Shading device: Position control in accordance with illuminance, indoor air temperature, minimum solar radiation, and working hours

(f) Shading device: Position control based on the solar radiation on the exterior side of windows, indoor air temperature, minimum solar radiation and working hours.

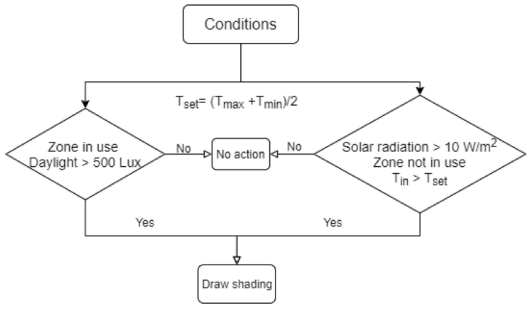

(g) Shading device: Position control based on illuminance

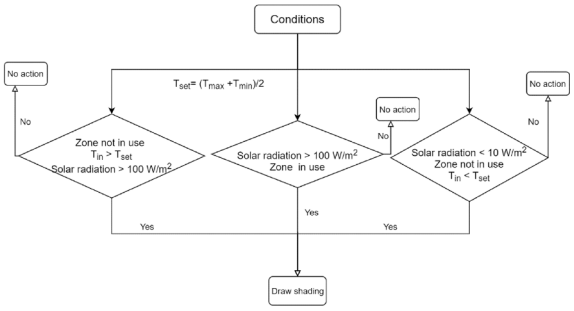

(h) Shading device: Position control based on solar radiation on the exterior side of windows

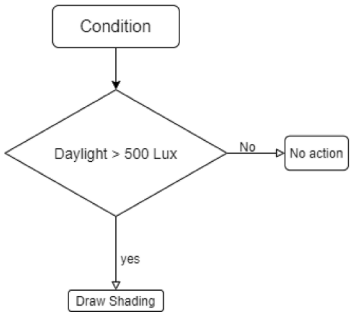

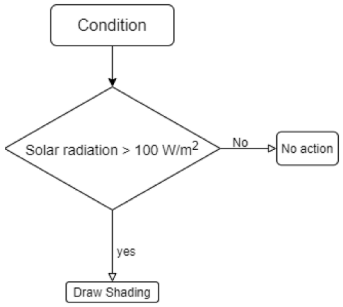

Fig. 4. Flow diagram of different control methods for automatic window opening and control of the shading device.

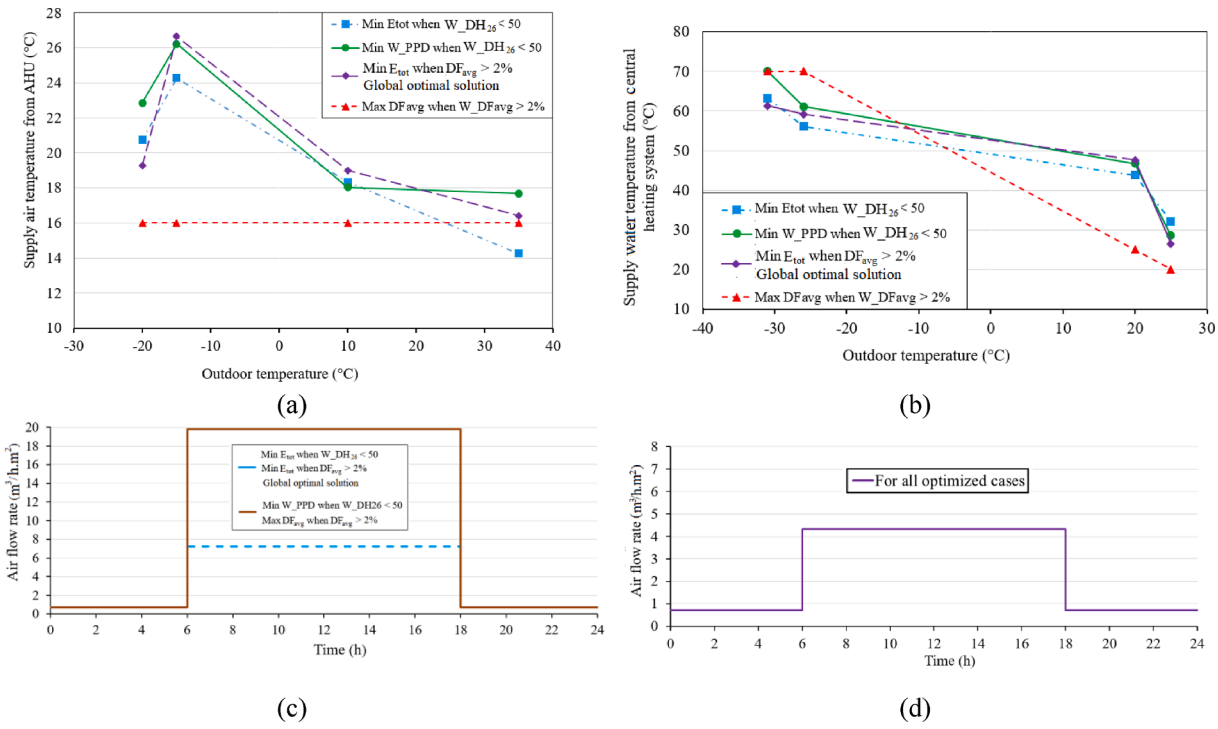

Fig. 5. Optimal (a) supply air temperature profile from AHU, (b) supply water temperature, (c) ventilation supply airflow rate during the cooling season, and (d) ventilation supply airflow rate during the heating season.

$$\gamma = \frac{self-conumption\ of\ generated\ electricity}{on-site\ electricity\ generation} = \frac{E_{self.use}}{\sum_{m=1}^{12} E_{el.prod.}} \quad (9)$$

In the above-mentioned equations, the absolute sign was used, because the produced energy was given a negative sign and the used energy was given a positive sign. For hourly calculations, the number of samples was changed to 8760 for the entire year. The PV module had an average efficiency of 18% for monocrystalline PV cells [69]. Furthermore, a tilt angle of 35°, the optimal PV tilt angle in Oslo climate, [70] module quality loss of 1.2%, and inverter operation loss of 8% were considered for the PV system, which gives a yearly average PR of 67% [70]. The weighting factor 2.3 [71] was also considered for imported and exported primary energy for ZEB balance calculations.

It is worth mentioning that an important point regarding the ZEB calculations in this study was to significantly take advantage of the self-consumption of generated electricity on-site. It is economically preferable to use the generated electricity directly in the building instead of exporting it to the grid. This is because the grid owner would only pay the electricity price (spot-price) plus a feed-in tariff, but not the grid-tariff, for the exported electricity. Therefore, the price of the sold electricity would only be about half the total price for the imported electricity.

4. Results

4.1. Optimization results

In the first part of this section, the optimization results are presented and analyzed considering thermal comfort and visual comfort constraint functions. Afterwards, the ZEB analysis was conducted for the optimal solution.

Table 7 shows the best set of input parameters after the optimization. Lighting performance and heat exchanger efficiency were always set to the lowest and the largest values for all the optimization scenarios, respectively. The reason was that the improvement of lighting system and heat exchanger efficiency decreased the building energy use with trivial impact on the visual and thermal comfort conditions. Regarding the window to floor area ratio, the maximum possible value was chosen during optimization when the visual comfort was the matter of concern. However, a moderate value was selected for the minimum energy use and the maximum thermal comfort cases implying that this parameter was a conflicting factor for maximizing visual comfort and thermal comfort and minimizing energy use simultaneously. Among the U-values of building façade, external wall retrofitting with low U-value was prioritized for all the scenarios, except the case with the maximum visual comfort as this parameter did not have any impact on the daylight. The roof renovation to lowest U-value was the preference of the scenarios with thermal comfort satisfaction.

Regarding shading device and window opening, the control methods based on the temperature and solar radiation setpoints (Condition (b) and Condition (h) in Fig. 4) were the preferred options for the global optimal solution, while none of control methods for window opening was desirable in terms of providing the best thermal comfort conditions. It is also interesting to note that the simple control method (Condition (h) in Fig. 4) for shading device was selected in the majority of the optimization cases except the cases concerning discomfort hours inferring that a complicated control method did not necessarily ensure an indoor comfort condition. Overall, comparison of the window opening and the shading device control methods indicate that the solar radiation and the indoor temperature parameters were the most effective factors in controlling the dynamic shading device and the window opening. This was especially achieved when different setpoints were considered for the same parameter, for example solar radiation, for controlling the shading and window opening. The reason could be justified by the coincidence of solar shading and window opening activation. In fact, selecting the same parameters, but with different setpoints, for the control methods of shading device and window opening ascertained that the shading would not be drawn when the windows were open, and the best performance of both shading and window opening was achieved.

Fig. 5 shows the optimal supply air temperatures and supply airflow rate setpoints in the AHU and the supply water temperature from the central heating system. A different trend is observed in the Max DF_{avg}

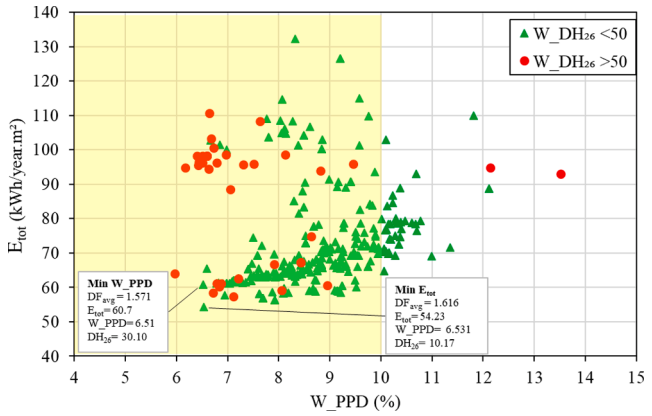

Fig. 6. Scatter plot of optimization solutions filtered only by thermal comfort constraint.

case because modifying the supply air temperature setpoints did not affect maximizing visual comfort (see Fig. 5(a) and (b)). However, for other cases in which minimizing the energy use and maximizing the thermal comfort were the primary optimization objectives, a similar variation patterns of the supply air temperature from the AHU, and the supply water temperature from the central heating system were selected for various cases after the optimization of the reference building (Fig. 5 (a) and (b)).

Furthermore, the lowest air flow rate was chosen for the cases in which minimizing the building energy use was the primary goal, while the highest air flow rate was selected for visual and thermal comfort as the main objective during the cooling season, as shown in Fig. 5 (c). The same air flow rate, as the reference case, was chosen for all the cases in heating season, as shown in Fig. 5 (d). It implies that adjusting the supply air temperature in the AHU could both minimize the building energy use and satisfy the thermal comfort requirement for all the cases resulting in no change in the air flow rate pattern during the heating season.

Fig. 6 shows all the simulated cases after optimization when the thermal comfort was the only constraint. Most of the cases could satisfy both the thermal discomfort hours and the average PPD requirements. The minimum energy use when the thermal comfort was the only constraint was obtained around 54 kWh/(m^2.year) and the energy use for the case with the minimum W_PPD was achieved around 61 kWh/

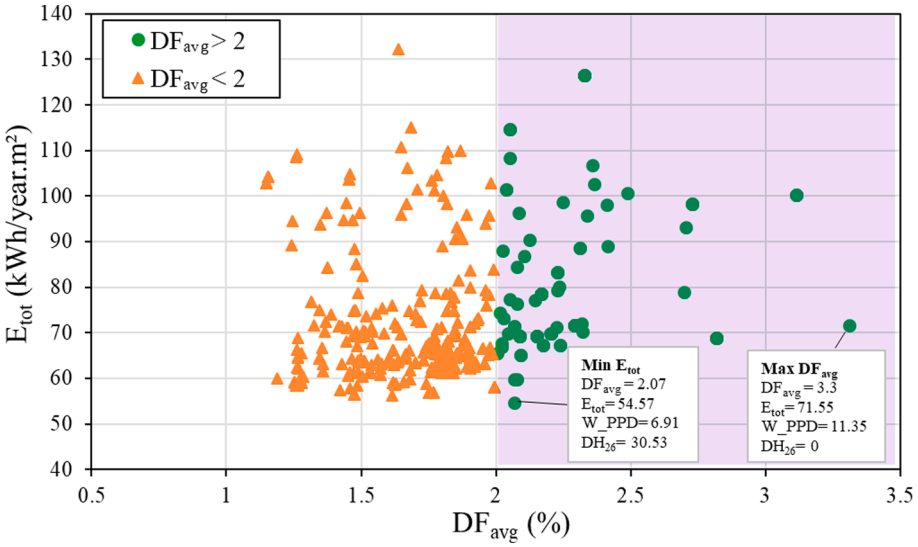

Fig. 7. Scatter plot of optimization solutions filtered only by visual comfort constraint.

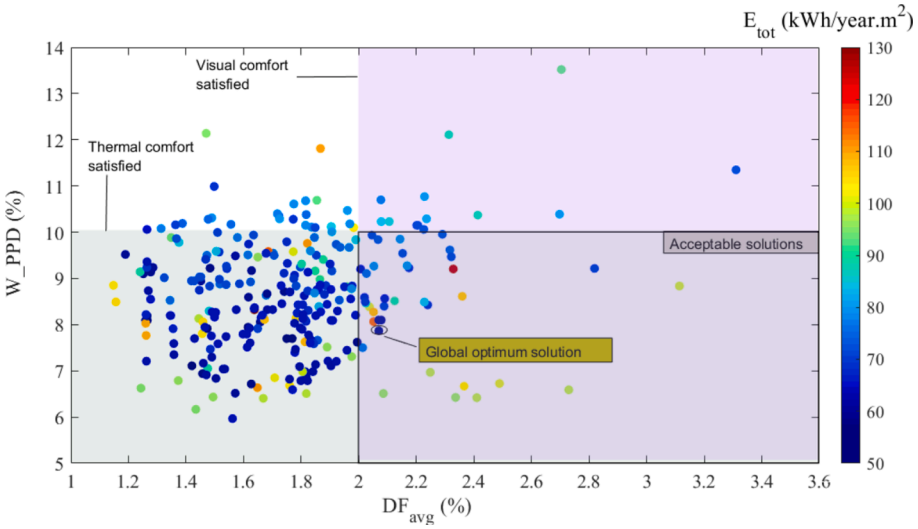

Fig. 8. W_PPD vs DF$_{avg}$ for different values of E$_{tot}$ objective function.

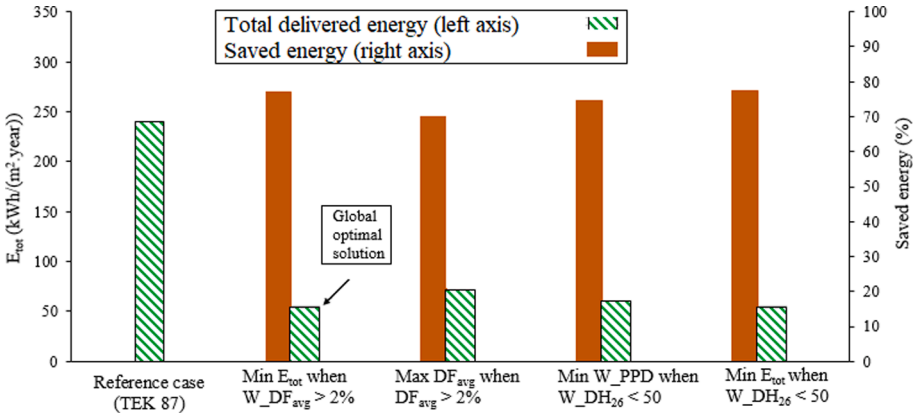

Fig. 9. Total delivered energy for different optimized scenarios.

(m^2.year). Comparing the optimized set of input variables for these two specific cases, see Table 6, may justify the results. The best quality of window (the lowest U-value) could not be used to reach the minimum average PPD due to increase of discomfort hours during the summer. In this respect, a slight decrease in the minimum average PPD in the Min W_PPD case resulted in a dramatic increase in the overheating hours, around 3 times, and the cooling energy use, around 1.2 times more than the Min E_{tot} case. This can support the importance of performing optimization to find an optimal solution in retrofitting studies.

Fig. 7 shows the scatter plot related to the energy use of all the optimized solutions considering only daylight factor constraint. Compared to the thermal comfort (see Fig. 6), fewer solutions could satisfy the daylight factor requirements implying that achieving visual comfort was more challenging than thermal comfort when retrofitting a building. It also indicates that the thermal comfort and visual comfort are two conflicting factors to reach low building energy use. For example, the selection of window to floor area ratio in different scenarios was the most important parameter on the daylight factor. This infers that a larger ratio was more desirable in terms of daylight factor (visual comfort condition) whereas smaller ratio was more favorable when the thermal comfort was the matter of concern. This in turn could affect the choice of other input parameters by the optimization engine in order to achieve the minimum building energy use. Fig. 7 also displays that, The minimum total energy use was obtained around 55 kWh/(m^2.year) when the results were only filtered by the visual comfort. Referring the optimized input parameters in Table 6, it infers that window to floor area ratio was the most sensitive parameter to be optimized so that a small increase to satisfy the visual comfort (Min E_{tot} when $DF_{avg} > 2\%$) led to the change in all other input parameters including shading device control methods to reach the minimum possible energy use. The consequence was, however, a significant increase in the discomfort hours (see Fig. 7).

Taking both visual and thermal comfort constraint functions into account, fewer solutions fell within the acceptable solution area (see Fig. 8). The global optimal solution was the same as the case with minimum energy use filtered by the average daylight factor (Min E_{tot} when $DF_{avg} > 2\%$). It is interesting to point out that the cases with a low W_PPD and high DF_{avg} values had a relatively high energy use (yellow and green points in the lower part in the acceptable solutions area). However, the solutions with less energy use fell within the thermal comfort satisfied area (dark blue points in the lower part in the thermal comfort satisfied area) emphasizing the difficulty of finding an optimal solution when considering both thermal and visual comfort filters. The reason was that a fewer number of parameters (mainly window to floor area ratio and partly glazing type) affected daylight factor than the thermal comfort.

The corresponding energy use for different optimized scenarios is presented in Fig. 9. Compared to the reference case, the total delivered energy reduced dramatically after optimization, 77.4% for the case with the minimum E_{tot} filtered by discomfort hours (regardless visual comfort) and 77.2% for the global optimal solution. As a matter of fact, this considerable energy saving would be more limited if the cost effectiveness of retrofitting option was also taken into account. However, the proposed optimization process in this paper provides informative insights on the importance of various control methods of window opening, shading device, and HVAC setpoints adjustment in the improvement of building energy performance, which impose almost low investment cost during retrofitting process.

Fig. 10 shows the annual operative temperature variation in one of the worst zones, for example, C.O.16 cell office see Fig. 2, in terms of the indoor operative temperature fluctuation before and after the optimization and according to NS-EN 15251:2007 comfort categories for office buildings [64]. The three categories limits in Fig. 10 were implemented according to the standard for acceptable indoor operative temperature in office buildings equipped with a cooling system. In addition to a large energy saving after the optimization, see Fig. 9, the operative temperature was also improved during both winter and summer operation. In this regard, the number of hours met the comfort category II (recommended for office buildings) considerably increased after the optimization, up to 10 times more than the reference case. Comparing different cases show that the best operative temperature profile, in terms of number of hours met the comfort category II, occurred in the Min W_PPD (Case (c) in Fig. 10) with around 6,573 h. The consequence was a higher delivered energy and higher number of discomfort hours (W_DH_{26}), especially during September and October, than the Min $E_{tot,}$ $DH_{26} < 50$ (case (b) in Fig. 10). Furthermore, referring to Table 7, it can be noted that a shading control method based on the combination control of solar radiation, daylight, and the indoor temperature setpoints led to the best performance in terms of satisfactory operative temperature.

4.2. Results of ZEB balance

Fig. 11 illustrates the process to reach ZEB balance through the imported and exported primary energy balance. Firstly, a large amount of energy saving, around 81%, in primary imported energy was achieved during optimization and the ZEB balance was then achieved by exporting electricity from onsite production.

Therefore, the required PV panel area to reach ZEB level was around 1,352 m^2 for the global optimal solution and around 5,960 m^2 for the reference case, if no optimization was performed. Furthermore, as the roof area was around 1,000 m^2, these optimized PV might be placed on the roof somehow. But, without optimization, it would be completely impossible or not feasible.

Fig. 12 shows the monthly variation of electricity portion in ZEB analysis in terms of export/production and import/consumption. The maximum electricity production for both the reference and the

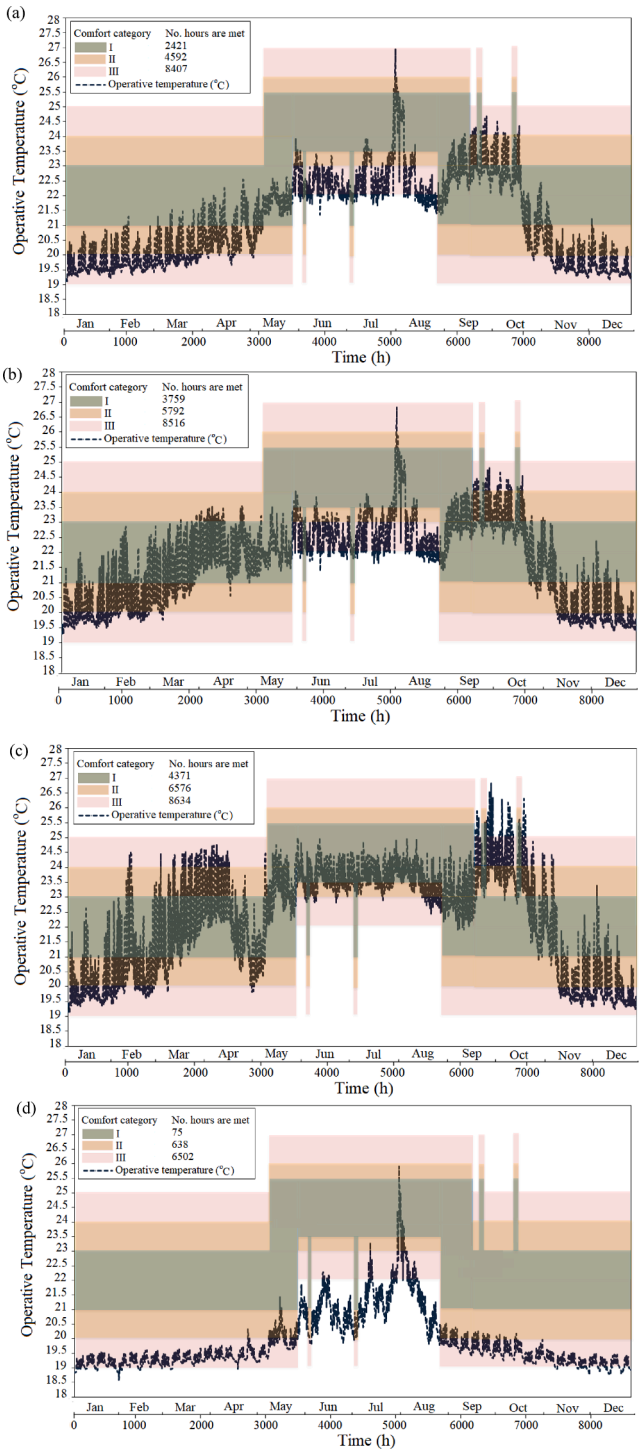

Fig. 10. Thermal comfort analysis in terms of operative temperature according to NS-EN 15251:2007 for (a) Min E_{tot} when $DF_{avg} > 2\%$, (b) Min E_{tot} when $DH_{26} < 50$, (c) Min W_PPD when $DH_{26} < 50$, and (d) reference cases for the C. O.16 cell office located in the third floor.

optimized cases was achieved during summer time, due to high solar radiation intensity. Consequently, a significant amount of electricity was imported during the winter, and a high portion of electricity was exported during the summer.

Additionally, there was still some amount of imported electricity even during summer, even though the electricity produced by PV was tried to be self-consumed as much as possible. It can be observed in Fig. 13 that the optimized case internally consumed nearly half of the

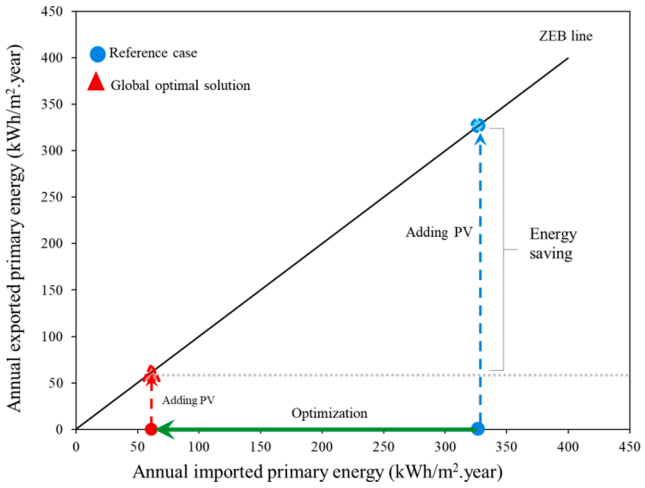

Fig. 11. ZEB analysis process in terms of exported and imported primary energy use.

generated electricity by PV panels. More precisely, considering the supply cover factor as defined in Eq. (9), 54% of the on-site produced electricity on a monthly basis, and 51% of that on an hourly basis, was self-consumed in the building.

An important point regarding ZEB balance is that it is economically preferable to use the generated electricity directly in the building (self-consumption) instead of exporting it to the grid. This is because the power company will only pay for the electricity price (Spot-price) plus a feed-in tariff, but not for the grid-tariff, for the exported electricity. Therefore, the price for the exported electricity will be only about the half price for the imported electricity.

5. Discussion

The findings in the result section pose some issues for discussion about the optimization process, both with respect to the adopted method and to the obtained results.

Employing IDA-ICE provided the possibility to implement all optimization input parameters, including the shading and window opening control methods, and the constraint and objective function through the parametric tab and GS interface in the software, which take advantage of a graphical user interface for applying functions and parameters. In addition, adopting the PSO algorithm, coupled with GS interface of the dynamic simulation IDA-ICE software, allowed decreasing the number of simulations by excluding those that did not meet the visual and thermal comfort constraint criteria. In this regard, all combinations of the 15 considered parameters, each of them with different alternatives, were in total 1.07×10^{18} cases. By using the optimization, such a vast number of simulation cases were dropped to only 1,900 cases, which were performed by IDA-ICE software. Nevertheless, since both energy and daylight simulations were run for each case with complicated window opening and shading control methods, the computational time increased remarkably.

With regard to the findings related to the energy savings due to the building retrofit measures, it is interesting to also discuss about the cost effectiveness of the building retrofit interventions. Since a substantial reduction of building energy use was achieved, compared to the reference building, through the optimization process, the operational cost would also decrease. This noticeable energy saving might not be reached if the cost effectiveness of retrofit measures was also taken into consideration, due to the investment costs of using extra systems and materials. However, we proposed a large group of retrofit measures, including various control methods of window opening, shading device, and HVAC setpoints adjustment, which could improve the building energy performance with almost low investment cost during retrofitting

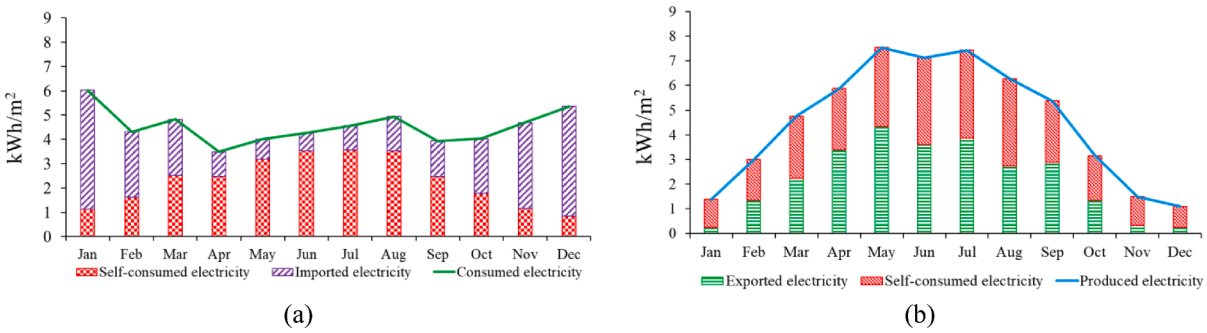

Fig. 12. Monthly variation of electricity portion in ZEB analysis in terms of (a) export/production and (b) import/consumption for the global optimal solution.

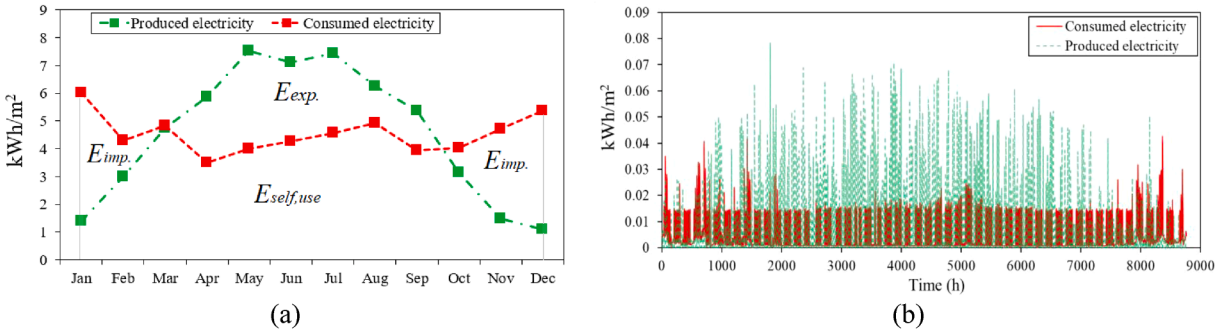

Fig. 13. (a) Monthly and (b) hourly production and consumption electricity with areas for ZEB balance.

process. This could imply that the reduction of operational cost due to enhancement of building energy performance might be dominant in the life cycle cost of the building retrofitting.

6. Conclusion

This paper focused on the retrofitting of building performance in terms of energy use and thermal comfort and visual comfort criteria. For this purpose, an inclusive optimization approach integrating building envelope, glazing parameters, HVAC setpoints, shading device, and window opening control methods was adopted. The shading and window opening control strategies were implemented using various control methods including the indoor air temperature, the CO_2 level, the daylight level, the wind velocity, and direct solar radiation on the façade. All these control methods were developed through the control macros in IDA-ICE, while the visual and thermal comfort constraints were implemented and linked to GenOpt (optimization tool) using Graphical Script interface in IDA-ICE. The main aim was to minimize the delivered energy to an office building, located in the Nordic climate, while meeting the thermal and visual comfort requirements at the same time. Afterwards, a ZEB analysis was performed by integrating PV panels in the building site for on-site production of electricity.

The findings showed that the building energy use for space heating and space cooling could be significantly reduced through optimization process, up to 77%, compared to the reference building case modelled in compliance with the Norwegian building regulation TEK87. Moreover, both visual and thermal comfort requirements, according to the Norwegian building regulation TEK17 and the standard NS-EN 15251:2007, were satisfied. In this regard, the optimal shading control method was based on solar radiation on the exterior side of the windows and the best performance regarding the window opening was attained when the control method was in accordance with indoor air temperature, direct solar radiation on the façade, and wind velocity setpoints, for the summer operation. Accordingly, the main factors in controlling shading devices and window opening were selected based on the indoor air temperature and the solar radiation parameters, but with different setpoints for these optimization input variables. The optimal shading material was Bisque venetian Blind slat. The other input parameters obtained for the global optimal solution included the best quality of envelope, except for the roof, and the highest efficiency of heat exchanger in the AHU. It was followed by the adjustment of the ventilation supply air temperature and the flow rate in the AHU and the supply water temperatures from the central heating plant to the local radiators. However, the most challenging optimization design variable to select was the window to floor area ratio because it influenced the thermal and visual comfort in an opposite way. In other words, it was difficult to find an optimal ratio satisfying both thermal and visual comfort requirements because it would affect the selection of other design variables such as window opening and shading control methods, which had impact on the thermal comfort and building energy use. This could signify the role of optimization methods in feasible studies of building retrofitting with large number of design variables. Furthermore, the ZEB analysis revealed that for the optimal solution, the required PV panel area was around 1,352 m^2 and for the reference case it was around 5,960 m^2 if no retrofitting was performed.

Future work on the optimization process can investigate the improvement of building performance equipped with all-air system in terms of energy use and thermal and visual comfort criteria. Additionally, thermal comfort and visual comfort can be assessed in further detail through conducting daylight and CFD simulations as a post processing step. It is an interesting case to compare the spatial distribution of thermal and visual comfort indexes instead of only evaluating an average value of these parameters before and after optimization. It is specifically important that a dynamic visual comfort index such as daylight autonomy or useful daylight illuminance is applied, as using the average daylight factor is not an appropriate way to optimize the position of shading device.

Declaration of Competing Interest

Hereby, the authors confirm that the paper does not have any conflicts of interest and any financial and personal relationships with other

people or organizations.

Appendix

The window opening in IDA-ICE was modelled based on the following equation [60]:

$$A_{eff} = C_d \cdot W \cdot H \tag{10}$$

where the discharge coefficient, C_d, was selected as default value set to 0.65. It should be noted that the window opening percentage was associated with the effective opening area of the window in Eq. (10).

Table 8
Optical properties of various shading device materials.

Shading slat materials	Visible transmittance	Visible outside reflectance	Visible inside reflectance	Emissivity
Generic outside blind slat	0	0.35	0.35	0.9
Marine venetian blind slat	0	0.0725	0.0725	0.9
Celery venetian blind slat	0	0.331	0.331	0.9
Opaque light–dark colored slat	0	0.7	0.4	0.9
Pewter venetian blind slat	0	0.364	0.364	0.9
Opaque white colored slat	0	0.7	0.7	0.9
Mocha venetian blind slat	0	0.323	0.323	0.9
Bisque venetian Blind slat	0	0.549	0.549	0.9
White venetian Blind slat	0	0.743	0.743	0.9

Table 9
Algorithm parameters for the optimization process.

Algorithm type	Algorithm parameter	Value
PSO	Neighbourhood topology	Von Neumann
	Neighbourhood size	5
	Number of particles	10
	Seed	50
	Number of generations	20
	Cognitive acceleration	2.8
	Social acceleration	1.3
	Maximum velocity discrete	4
	Constriction gain	0.5

References

[1] I. Artola, K. Rademaekers, R. Williams, J. Yearwood, Boosting building renovation: What potential and value for Europe, Study for the iTRE Committee, Commissioned by DG for Internal Policies Policy Department A (2016) 72.
[2] Y. Saheb, A. Saussay, C. Johnson, A. Blyth, A. Mishra, T. Gueret, Modernising Building Energy Codes, (2013).
[3] O.d.c.e.d.d. économiques, Transition to sustainable buildings: strategies and opportunities to 2050, OECD Publishing2013.
[4] DIRECTIVE (EU) 2018/844 of the European parliament and of the council of 30 May 2018 amending Directive 2010/31/EU on the energy performance of buildings and Directive 2012/27/EU on energy efficiency (Text with EEA relevance), Official Journal of the European Union, 2018.
[5] Nord N. Building energy efficiency in cold climates. Encyclopedia of Sustainable Technologies 2017:149–57.
[6] Ferrara M, Filippi M, Sirombo E, Cravino V. A simulation-based optimization method for the integrative design of the building envelope. Energy Proc 2015;78:2608–13.
[7] Ferrara M, Sirombo E, Fabrizio E. Automated optimization for the integrated design process: the energy, thermal and visual comfort nexus. Energy Build 2018;168:413–27.
[8] Pasichnyi O, Levihn F, Shahrokni H, Wallin J, Kordas O. Data-driven strategic planning of building energy retrofitting: the case of Stockholm. J Cleaner Prod 2019;233:546–60.
[9] Fan C, Yan D, Xiao F, Li A, An J, Kang X. Advanced data analytics for enhancing building performances: from data-driven to big data-driven approaches. Build Simul 2020.
[10] Hashempour N, Taherkhani R, Mahdikhani M. Energy performance optimization of existing buildings: a literature review. Sustain Cities Soc 2020;54.
[11] Ascione F, Bianco N, Mauro GM, Vanoli GP. A new comprehensive framework for the multi-objective optimization of building energy design: Harlequin. Appl Energy 2019;241:331–61.
[12] Grillone B, Danov S, Sumper A, Cipriano J, Mor G. A review of deterministic and data-driven methods to quantify energy efficiency savings and to predict retrofitting scenarios in buildings. Renew Sustain Energy Rev 2020;131:110027.
[13] Ali U, Shamsi MH, Bohacek M, Hoare C, Purcell K, Mangina E, et al. A data-driven approach to optimize urban scale energy retrofit decisions for residential buildings. Appl Energy 2020;267:114861.
[14] Lin Y-H, Lin M-D, Tsai K-T, Deng M-J, Ishii H. Multi-objective optimization design of green building envelopes and air conditioning systems for energy conservation and CO2 emission reduction. Sustain Cities Society 2021;64:102555.
[15] Rosso F, Ciancio V, Dell'Olmo J, Salata F. Multi-objective optimization of building retrofit in the Mediterranean climate by means of genetic algorithm application. Energy Build 2020;216.
[16] Lu S, Li J, Lin B. Reliability analysis of an energy-based form optimization of office buildings under uncertainties in envelope and occupant parameters. Energy Build 2020;209.
[17] Ascione F, Bianco N, Iovane T, Mauro GM, Napolitano DF, Ruggiano A, et al. A real industrial building: modeling, calibration and Pareto optimization of energy retrofit. J Build Eng 2020;29:101186.
[18] Chang S, Castro-Lacouture D, Yamagata Y. Decision support for retrofitting building envelopes using multi-objective optimization under uncertainties. J Build Eng 2020;32:101413.
[19] Li H, Wang S. Coordinated optimal design of zero/low energy buildings and their energy systems based on multi-stage design optimization. Energy 2019;189:116202.
[20] Si B, Wang J, Yao X, Shi X, Jin X, Zhou X. Multi-objective optimization design of a complex building based on an artificial neural network and performance evaluation of algorithms. Adv Eng Inf 2019;40:93–109.
[21] Ascione F, Bianco N, Mauro GM, Napolitano DF. Retrofit of villas on Mediterranean coastlines: Pareto optimization with a view to energy-efficiency and cost-effectiveness. Appl Energy 2019;254:113705.
[22] Ascione F, Bianco N, Mauro GM, Napolitano DF, Vanoli GP. Weather-data-based control of space heating operation via multi-objective optimization: application to Italian residential buildings. Appl Therm Eng 2019;163:114384.
[23] Ilbeigi M, Ghomeishi M, Dehghanbanadaki A. Prediction and optimization of energy consumption in an office building using artificial neural network and a genetic algorithm. Sustain Cities Soc 2020;61:102325.
[24] Bui D-K, Nguyen TN, Ghazlan A, Ngo N-T, Ngo TD. Enhancing building energy efficiency by adaptive façade: a computational optimization approach. Appl Energy 2020;265:114797.
[25] Nasruddin Sholahudin, Satrio P, Mahlia TMI, Giannetti N, Saito K. Optimization of HVAC system energy consumption in a building using artificial neural network and multi-objective genetic algorithm. Sustain Energy Technol Assess 2019;35:48–57.
[26] Guo R, Heiselberg P, Hu Y, Zhang C, Vasilevskis S. Optimization of night ventilation performance in office buildings in a cold climate. Energy Build 2020;225:110319.
[27] Lu Y, Wang S, Zhao Y, Yan C. Renewable energy system optimization of low/zero energy buildings using single-objective and multi-objective optimization methods. Energy Build 2015;89:61–75.
[28] Wu R, Mavromatidis G, Orehounig K, Carmeliet J. Multiobjective optimisation of energy systems and building envelope retrofit in a residential community. Appl Energy 2017;190:634–49.

[29] Hirvonen J, Jokisalo J, Heljo J, Kosonen R. Towards the EU emissions targets of 2050: optimal energy renovation measures of Finnish apartment buildings. Int J Sustain Energy 2018;38(7):649–72.
[30] Ferrara M, Rolfo A, Prunotto F, Fabrizio E. EDeSSOpt – Energy Demand and Supply Simultaneous Optimization for cost-optimized design: application to a multi-family building. Appl Energy 2019;236:1231–48.
[31] Taveres-Cachat E, Lobaccaro G, Goia F, Chaudhary G. A methodology to improve the performance of PV integrated shading devices using multi-objective optimization. Appl Energy 2019;247:731–44.
[32] Fang Y, Cho S. Design optimization of building geometry and fenestration for daylighting and energy performance. Sol Energy 2019;191:7–18.
[33] P. Pilechiha, M. Mahdavinejad, F. Pour Rahimian, P. Carnemolla, S. Seyedzadeh, Multi-objective optimisation framework for designing office windows: quality of view, daylight and energy efficiency, Applied Energy 261 (2020).
[34] Kirimtat A, Krejcar O, Ekici B, Fatih Tasgetiren M. Multi-objective energy and daylight optimization of amorphous shading devices in buildings. Sol Energy 2019; 185:100–11.
[35] Yi YK. Building facade multi-objective optimization for daylight and aesthetical perception. Build Environ 2019;156:178–90.
[36] Naderi E, Sajadi B, Behabadi MA, Naderi E. Multi-objective simulation-based optimization of controlled blind specifications to reduce energy consumption, and thermal and visual discomfort: case studies in Iran. Build Environ 2020;169.
[37] Magnier L, Haghighat F. Multiobjective optimization of building design using TRNSYS simulations, genetic algorithm, and Artificial Neural Network. Build Environ 2010;45(3):739–46.
[38] Hong T, Kim J, Lee M. A multi-objective optimization model for determining the building design and occupant behaviors based on energy, economic, and environmental performance. Energy 2019;174:823–34.
[39] Grygierek K, Ferdyn-Grygierek J. Multi-objective optimization of the envelope of building with natural ventilation. Energies 2018;11(6).
[40] Niemelä T, Levy K, Kosonen R, Jokisalo J. Cost-optimal renovation solutions to maximize environmental performance, indoor thermal conditions and productivity of office buildings in cold climate. Sustain Cities Soc 2017;32:417–34.
[41] Sghiouri H, Mezrhab A, Karkri M, Naji H. Shading devices optimization to enhance thermal comfort and energy performance of a residential building in Morocco. J Build Eng 2018;18:292–302.
[42] Ascione F, Bianco N, Maria Mauro G, Napolitano DF. Building envelope design: Multi-objective optimization to minimize energy consumption, global cost and thermal discomfort. Application to different Italian climatic zones. Energy 2019; 174:359–74.
[43] Ascione F, Bianco N, De Masi RF, Mauro GM, Vanoli GP. Energy retrofit of educational buildings: transient energy simulations, model calibration and multi-objective optimization towards nearly zero-energy performance. Energy Build 2017;144:303–19.
[44] Tian ZC, Chen WQ, Tang P, Wang JG, Shi X. Building energy optimization tools and their applicability in architectural conceptual design stage. Energy Procedia 2015; 78:2572–7.
[45] M. Wetter, GenOpt (R), generic optimization program, User Manual, Version 2.0. 0, (2003).
[46] M. Palonen, M. Hamdy, A. Hasan, MOBO a new software for multi-objective building performance optimization, BS2013, France, 2013.
[47] Y. Zhang, Use jEPlus as an efficient building design optimisation tool, CIBSE ASHRAE Technical Symposium, Imperial College, London UK 2012.
[48] C. Christensen, R. Anderson, S. Horowitz, A. Courtney, J. Spencer, BEopt™ Software for Building Energy Optimization: Features and Capabilities, National Renewable Energy Lab. (NREL), Golden, CO (United States), United States, 2006.
[49] Chantrelle FP, Lahmidi H, Keilholz W, Mankibi ME, Michel P. Development of a multicriteria tool for optimizing the renovation of buildings. Appl Energy 2011;88 (4):1386–94.
[50] Schwartz Y, Raslan R, Mumovic D. Implementing multi objective genetic algorithm for life cycle carbon footprint and life cycle cost minimisation: a building refurbishment case study. Energy 2016;97:58–68.
[51] Karaguzel OT, Zhang R, Lam KP. Coupling of whole-building energy simulation and multi-dimensional numerical optimization for minimizing the life cycle costs of office buildings. Build Simul 2013;7(2):111–21.
[52] Delgarm N, Sajadi B, Delgarm S. Multi-objective optimization of building energy performance and indoor thermal comfort: a new method using artificial bee colony (ABC). Energy Build 2016;131:42–53.
[53] Asadi E, da Silva MG, Antunes CH, Dias L. A multi-objective optimization model for building retrofit strategies using TRNSYS simulations, GenOpt and MATLAB. Build Environ 2012;56:370–8.
[54] Arabzadeh V, Jokisalo J, Kosonen R. A cost-optimal solar thermal system for apartment buildings with district heating in a cold climate. Int J Sustain Energy 2018;38(2):141–62.
[55] Statistics Norway, 2019, https://www.ssb.no/en/bygg-bolig-og-eiendom/statistikker/bygningsmasse/aar. (Accessed 2019.
[56] Byggeforskrift- TEK 87, 1987.
[57] NS 3031, 2014, Calculation of energy performance of buildings - Method and data, Standard Norge, p. 100.
[58] Fang Y, Ding Y, Nord N. Data-driven analysis of occupancy and lighting patterns in office building in Norway. REHVA J 2019:64–9.
[59] ANSI/ASHRAE/IESNA.2007, Standard 90.1e2007 normative Appendix B: building envelope climate criteria.
[60] Bring A, Sahlin P, Vuolle M. Models for Building Indoor Climate and Energy Simulation. KTH, Stockholm, Sweden: Dept. of Building Sciences; 1999.
[61] G. Ward, R. Shakespeare, Rendering with Radiance: the art and science of lighting visualization, (1998).
[62] M. Rabani, H. Bayera Madessa, O. Mohseni, N. Nord, Minimizing delivered energy and life cycle cost using Graphical script: An office building retrofitting case, Applied Energy 268 (2020).
[63] Building Technical Regulations (TEK17) 2017, with guidance (in Norwegian), § 13-4. Thermal indoor climate.
[64] NS-EN 15251:2007- Indoor environmental input parameters for design and assessment of energy performance of buildings addressing indoor air quality, thermal environment, lighting and acoustics, Standard Norge, 2007.
[65] Sartori I, Napolitano A, Voss K. Net zero energy buildings: a consistent definition framework. Energy Build 2012;48:220–32.
[66] K. Voss, I. Sartori, R. Lollini, Nearly-zero, net zero and plus energy buildings, REHVA Journal, Dec (2012).
[67] I. Sartori, S.V. Løtveit, K.S. Skeie, Guidelines on energy system analysis and cost optimality in early design of ZEB, 2018, p. 65.
[68] Noris F, Musall E, Salom J, Berggren B, Jensen SØ, Lindberg K, et al. Implications of weighting factors on technology preference in net zero energy buildings. Energy Build 2014;82:250–62.
[69] Tiwari GN, Mishra RK, Solanki SC. Photovoltaic modules and their applications: a review on thermal modelling. Appl Energy 2011;88(7):2287–304.
[70] Madessa HB. Performance analysis of roof-mounted photovoltaic systems – the case of a norwegian residential building. Energy Proc 2015;83:474–83.
[71] NS-EN ISO 52000-1, Energy performance of buildings Overarching EPB assessment, Part 1: General framework and procedures, Standard Norge, 2017, p. 144.